Journal of Materials Chemistry A

Accepted Manuscript

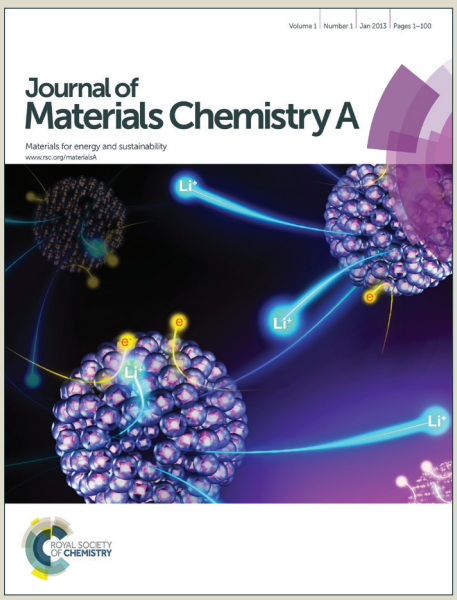

ROYAL SOCIETY OF CHEMISTRY

www.rsc.org/materialsA

TOC:

Color Graphic

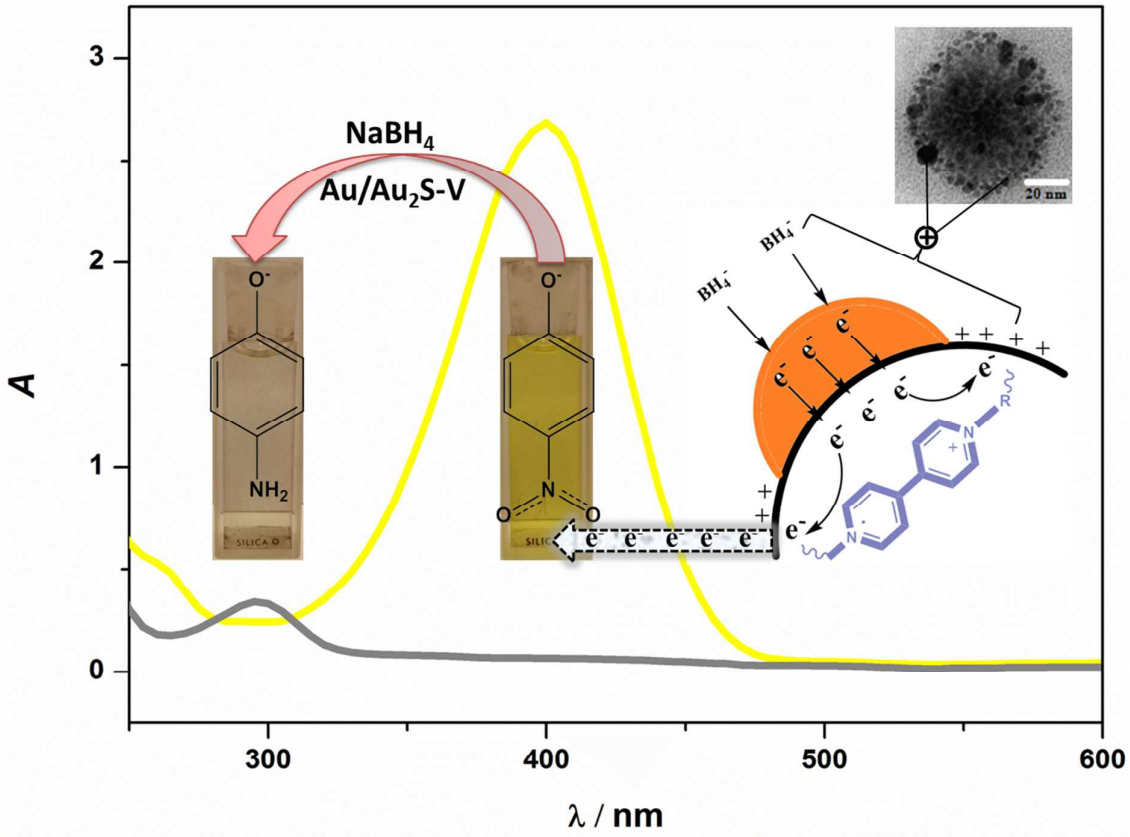

Text:

Synthesis of SDS stabilized flower like Au/Au_2S nanoparticles-viologen composite via one step dithionite reduction for efficient reduction of 4-nitrophenol to 4-aminophenol.

Journal Name

RSCPublishing

ARTICLE

One pot synthesis of Au/Au_2S nanoparticles-viologen hybrid composite for efficient catalytic applications

Cite this: DOI: 10.1039/x0xx00000x

Received 00th January 2012,
Accepted 00th January 2012

DOI: 10.1039/x0xx00000x

www.rsc.org/

Bhushan Gadgil[a,b,*], Pia Damlin[a], Antti Viinikanoja[a], Markku Heinonen[c] and Carita Kvarnström[a,*]

We report a facile one pot synthesis of Au/Au_2S multicomponent nanoparticles supported viologen (V) hybrid nanocomposite. Sodium dithionite was used as reducing agent for both Au and V precursors and SDS as stabilizing agent for Au nanoparticles in aqueous medium. Spectroscopy, microscopy and electrochemical measurements confirm the successful composite formation. The as prepared flower like composite showed excellent catalytic properties towards reduction of 4-nitrophenol (4-NP) to 4-aminophenol (4-AP). The catalytic activity factor of Au/Au_2S-V hybrid was highest in comparison to those reported for polymer supported Au nanoparticle catalysts. The enhanced catalytic performance can be attributed by the strong adsorption of 4-NP molecules on cationic V matrix and Au_2S nanoparticles surface along with effective donor-acceptor interactions between Au-Au_2S nanoparticles and V facilitating the electron transfer at the hybrid interface.

Introduction

In the past few years, there has been increasing amount of research concerned with multicomponent nanoparticles due to their novel functions which are not available in single component nanoparticles [1, 2]. Multicomponent nanoparticles represent an innovative approach to manufacture a new generation composite materials with improved properties that combine the desirable properties of the individual components via synergistic or complementary effects [3]. The attractive aspect of these multicomponent nanostructured assemblies is not only related to the combination of different properties and functionalities but also to the possibility of independently optimizing the dimensions and material parameters of the individual components. There have been several reports on the preparation of multicomponent nanoparticles including core-shell nanoparticles, segmented nanowires and particles coated with other particles [4, 5]. The few examples are CdSe/ZnS, Fe_2O_3/Fe_3O_4, FePt/ CdS, Au/ Fe_3O_4, Fe/FeS and Au/Au_2S. Such materials have great potential for a wide range of applications including magnetism, drug delivery, biomedical applications and contaminant removal [6, 7]. However, the controlled synthesis of multicomponent nanoparticles is still a matter of concern.

Gold (Au) nanoparticles have received considerable attention due to their unique physico-chemical properties and their importance in the field of catalysis [8]. The reactions of aqueous gold-sulfide ions system is well recognized due to the solubility of gold in hydrothermal fluids in geochemistry [9]. Lately, it has been found that Au coated Au_2S possess exceptional optical properties even in NIR region of the spectrum [10]. Meanwhile, these materials find their potential in biomedicine, optoelectronics and sensors [11-13]. When several research groups carried out a detailed investigation on the mechanism and evidence for Au-S bonding, they convinced that the unusual properties of Au particles in Au/Au_2S system are certainly due to sulfide species [14, 15]. Several sulfide minerals found their importance in wastewater remediation as well as removal of hazardous contaminants due to their strong adsorption properties [7, 16]. However, there has not yet been any report where Au_2S nanoparticles are utilized for catalytic applications.

Viologen materials are well known for their strong redox properties [17]. In our group, we fabricate viologen/polyviologen films via electrochemical reduction of cyanopyridine based monomers [18-20]. Kosower et al. proposed a simple reduction of 1-methyl-4-cyanopyridinium iodide to methyl viologen by dithionite in aqueous solution [21]. The method provides stable

viologen radicals with extraordinary redox properties. Few other properties of viologen materials to be mentioned are their electron accepting ability and porosity which have been utilized in applications like sensors and supercapacitors [22, 23]. For this reason, recently, the composite assemblies have been developed in combination with different electron donor materials like carbon nanostructures, metal nanoparticles etc [24-26].

In this paper, we describe a novel method for the preparation of Au/Au_2S nanoparticles deposited on viologen matrix via simultaneous reduction of Au and viologen precursor mixture using sodium dithionite ($Na_2S_2O_4$). Dithionite is a well-known reducing agent for the preparation of noble metal nanoparticles as well as for viologen/polyviologen materials through reduction of cyanopyridinium based monomers [7,27]. The method thus offers easy, one-step and rapid synthesis of Au/Au_2S-polyviologen hybrid nanostructured composite assembly. The as prepared composite consisting of Au/Au_2S multicomponent nanoparticles supported on V obviously stabilized by the net donor-acceptor interactions between the two. Owing to their electrostatic and non-covalent interactions, we envisioned that the hybrid nanocomposite could be beneficial in catalytic applications. For this reason, the catalytic performance of the composite has been tested for the reduction of 4-nitrophenol (4-NP) in an excess amount of $NaBH_4$. The unique feature of this Au/Au_2S-V composite catalyst is the easy preparation method, inexpensive catalyst support (V), lower amount of catalyst needed and fast catalytic conversion efficiency.

Experimental

Synthesis of Au/Au_2S-V hybrid nanocomposite

For a typical synthesis of Au/Au_2S-V hybrid nanocomposite, 1 mL (25 mM) of $HAuCl_4$ aqueous solution was mixed with 0.05 M SDS (sodium dodecyl sulfate) solution and stirred for 1h. Then 5 mL (0.5 M) of CNP [20] monomer aqueous solution was added to the above Au-SDS solution and stirred for 1h. Then 0.1 M of $Na_2S_2O_4$ (3 mL) solution was added dropwise for 15-20 mins. The resulting suspension was additionally stirred for 4 h to homogenize the content. The final suspension was then washed with copious amount of water and centrifuged in order to remove unreacted SDS and excess dithionite. The washing and centrifuge process is carried out 4-5 times to ensure the purity of the product. The final product was collected as Au/Au_2S-V composite.

Characterizations

Transmission electron microscopy (TEM) images were obtained by a JEM 1400-Plus (JEOL, Japan) instrument with a 120 kV acceleration voltage. High-resolution transmission electron microscopy (HRTEM) with EDS was performed using a double aberration-corrected JEOL JEM-2200FS microscope. FTIR spectra of the samples were recorded with a Bruker VERTEX 70 FTIR spectrometer equipped with a Harrick VideoMVP™ diamond ATR accessory using a liquid nitrogen cooled MCT (broad-band) detector. For each spectrum, 128 interferograms were recorded at a spectral resolution of 4 cm^{-1}. Raman measurements were performed with Nicolet Nexus 870 FTIR instrument equipped with a FT Raman module, Nd:YAG NIR laser (1064 nm) and Ge detector. XRD measurements were carried out using a Huber G670 image plate Guinier camera with copper $K_{\alpha 1}$ radiation (λ=1.5406 Å). Data collection time was 30 min with 10 scans of the image plate. XPS measurements were recorded with a Perkin–Elmer PHI 5400 spectrometer using Mg K_α radiation (1253.6 eV) and the spectra were analyzed with the Unifit2009 software (Unifit Scientific Software GmbH, Leipzig, Germany). The cyclic voltammetry (CV) experiment was performed in a conventional three-electrode one-compartment cell operated by Autolab (PGSTAT101) work station. Catalytic reaction kinetics of 4-NP was performed using Agilent Cary 60 UV-Vis spectrophotometer.

Catalytic tests

To study the catalytic activity, 0.05 mg of Au/Au_2S-V nanocomposite was dispersed in 3 mL of 4-NP aqueous solution (0.1 mM). Then a freshly prepared aqueous solution of $NaBH_4$ (0.2 M) was added. The molar ratio of Au/4-NP/ $NaBH_4$ was kept at 1/20/15000. The reaction mixture was sampled at fixed intervals and transferred into a quartz cuvette. The absorption spectra were recorded to monitor the reduction process of 4-NP.

Results and Discussions

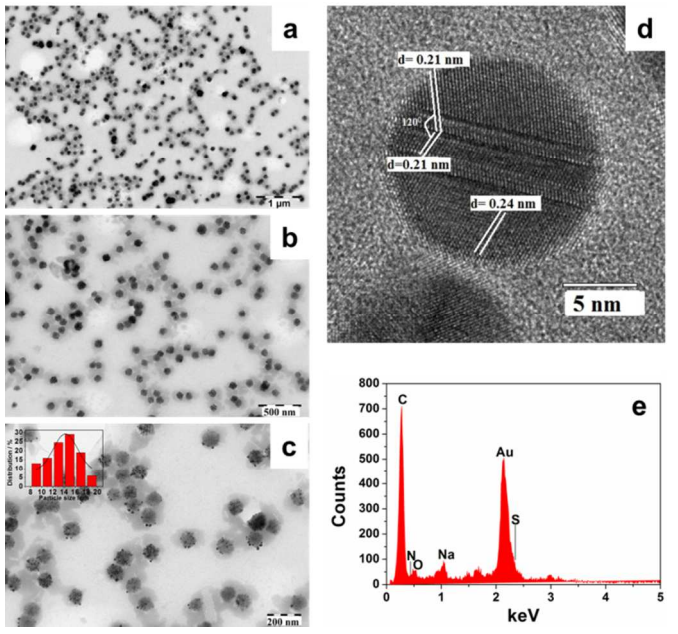

Fig. 1. a, b, c) TEM, **Inset of c):** Size distribution of Au/Au_2S nanoparticles in composite, **d)** HRTEM images of as synthesized Au/Au_2S-V nanocomposite and **e)** EDS pattern of Au/Au_2S-V nanocomposite.

Fig. 1a,b,c shows TEM images of Au/Au_2S-V nanocomposite which consists of cluster/ flower like morphology. The average size of the cluster is ~80 nm and the average particle size of Au/Au_2S nanoparticles is calculated to be ~15 nm. The HRTEM image (Fig. 1d) clearly shows lattice fringes with

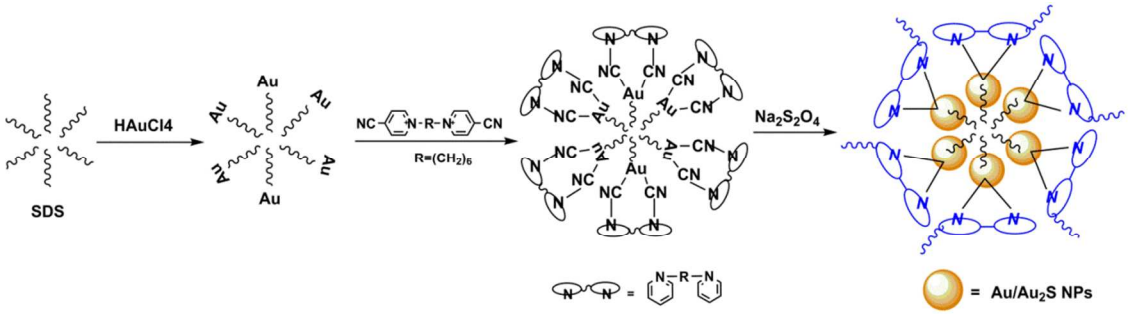

Scheme 1. Schematic illustration of Au/Au_2S-V nanocomposite fabrication.

oblique intersection at an angle of 1200 of the gold crystallites. Additionally, fringe widths were measured to be 2.1 Å and 2.4 Å, which corresponds to the (200) and (111) planes of gold, respectively. The EDS of Au/Au_2S-V **(Fig. 1e)** shows considerable amount of C, Au, S and N with Au:S ratio calculated to be 5:1, further confirming the successful composite formation.

Based on the TEM investigations, a possible route of fabrication of flower like Au/Au_2S-V composite is illustrated in **Scheme 1**. The negatively charged sulfate tail of SDS reacts with the Au^+ salt and forms AuDS. The further addition of cyanopyridine based monomer into the AuDS forms a hydrolyzed -CN complex with Au [28]. Finally, Au-CNP complex is reduced under continuous addition of dithionite. Dithionite is very unstable reductant and decomposes rapidly in aqueous solutions [29]. During decomposition, it releases hydrogen sulfide (H_2S) gas. When in contact with metal salts like Au, it readily precipitates as Au_2S while the remaining salt reduces to noble metallic Au (eq. 1-4).

$$2S_2O_4^{2-} + H_2O \rightarrow 2HSO_3^- + S_2O_3^{2-} \quad (1)$$

$$S_2O_4^{2-} + S_2O_3^{2-} + 2\,H_2O + H^+ \rightarrow H_2S + 3HSO_3^- \quad (2)$$

$$H_2S \rightarrow 2\,H^+ + S^{2-} \quad (3)$$

$$2Au^+ + S^{2-} \rightarrow Au_2S \quad (4)$$

Alongwith Au/Au_2S nanoparticles, the CNP monomer get reduced to V species. The conversion process of CNP to V is very fast and proceeds via one of the following two electron processes; either intramolecular electron transfer within sulphoxylate-4-cyanopyridinium ion complex (eq. 5) or reaction between SO_2^- anion radical and pyridinium ion (eq. 6).

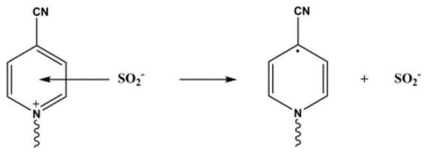

(5)

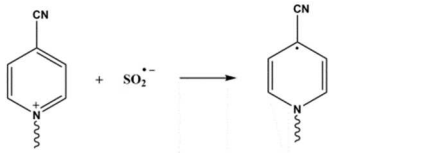

(6)

The final product can be viewed as Au/Au_2S nanoparticles surrounded by V matrix stabilized through Au-N complex shell [30].

The FTIR spectra of the composite shows successful formation of viologen from CNP based monomer **(Fig. 2a)**. As depicted, the monomer gives rise to a band at ~2240 cm^{-1} related to the –CN stretching vibrations [19] which eventually disappear after the composite formation. Moreover, a band due to –C=N ring stretching at 1642 cm^{-1} from CNP monomer became broader in the composite spectrum. A similar behavior can be seen in the –C-H deformation bands around 1100-1300 cm^{-1} which are sharp in the monomer spectrum but getting broader after the Au/Au_2S-V hybrid nanocomposite fabrication. The results suggest possible interactions between V and Au/Au_2S nanoparticles within the composite.

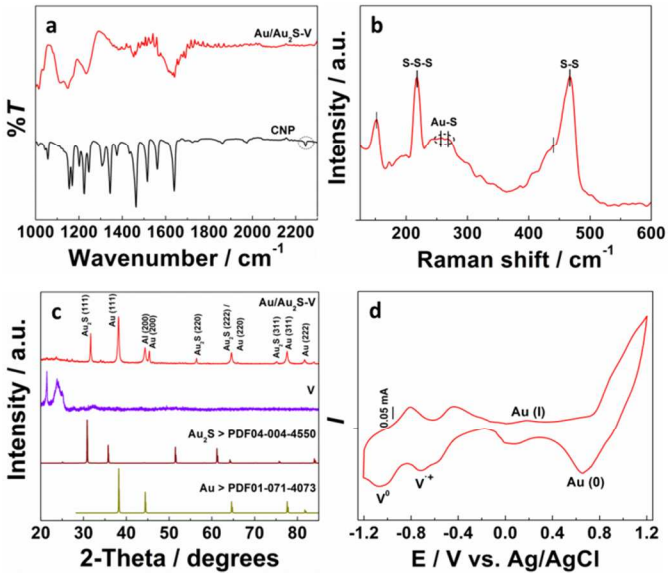

Fig. 2. a) FTIR spectra of CNP monomer and Au/Au_2S-V nanocomposite. **b)** Raman spectra of Au/Au_2S-V nanocomposite sol. **c)** XRD pattern of Au/Au_2S-V nanocomposite. **d)** Cyclic voltammogramm of Au/Au_2S-V deposited on tin oxide electrode in 0.1 M KCl aqueous electrolyte.

Raman spectra acquired from the composite sol displays bands due to the Au/Au_2S nanoparticles **(Fig. 2b).** The sharp bands at ~150 and 220 cm^{-1} can be ascribed to the S-S-S bending vibrations while those at ~440 and 460 cm^{-1} are attributable to S-S stretching [31]. The broad bands around ~250-270 cm^{-1} were due to the gold-sulphur stretching vibrations [32]. The weak Au-S interactions might be due to the V shell which surrounds the nanoparticles and weakens the Au-S bonding.

The formation of Au/Au_2S was further verified by their XRD patterns **(Fig. 2c)**. The (111), (220), and (222) reflection peaks of Au_2S can be clearly seen, confirming the formation of Au_2S nanoparticles [33]. Alongwith Au_2S, corresponding Au nanoparticle peaks can also be identified as (111), (200), and (311) reflections [34]. For comparison, Au and Au_2S reference library data is given. Moreover, the typical XRD pattern of viologen (between 20-27 degrees) is consistent in the composite, further confirming the contribution of viologen in the formed Au/Au_2S-V composite.

The CV of Au/Au_2S-V nanocomposite deposited on tin oxide electrode is represented in **Fig. 2d**. At the cathodic potential side, the CV comprises of a typical one electron transfer reaction showing two redox waves corresponding to the viologen (V) [35]. The broad peak at ~-0.5 to -0.7 V can be assigned to the viologen radical cation formation ($V^{\bullet+}$) with a corresponding anodic peak at -0.45 V. The next peak at -1.06 V analogues to the neutral viologen species (V^0) alongwith its anodic counterpart at -0.8 V. There is a slight shift in the V peaks to more negative potentials probably due to the possible synergistic interactions between viologen species and Au/Au_2S nanoparticles within the composite matrix. When scanned towards the anodic potential side, a broad redox response at 0.16 V can be visualized corresponding to the Au nanoparticles.

With further oxidation, Au forms oxide with corresponding reduction peak observed at ~0.7 V. These potential values correlate well with the values reported in the literature [36, 37].

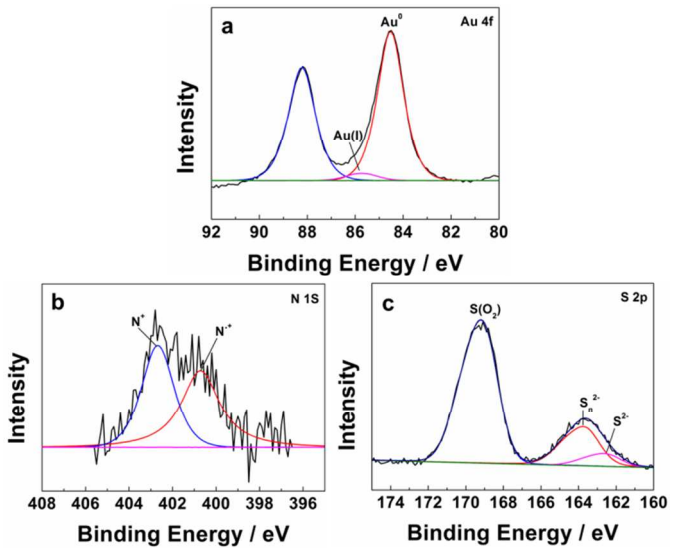

Fig. 3. a) Au 4f, **b)** S 2p and **c)** N 1s XPS spectra of the Au/Au_2S-V samples.

The XPS analysis was performed to identify the elemental contents in the sample **(Fig. 3).** The Au 4f bands are recognized as the metallic gold with Au $4f_{7/2}$ peak at 84.0 eV **(Fig. 3a)**. A very small contribution from Au(I) species can be observed at 85.6 eV [32]. The S 2p bands consists of a doublet at S $2p_{3/2}$ binding energies of 162.7 and 163.8 eV, representing monosulfide and polysulfide species **(Fig. 3b)**. The high peak at 169.2 eV can be ascribed to the oxide analogue of sulfur ($S(O_2)$) [38]. Similar spectra have been obtained from Au_2S nanoparticles and sulfur adsorbed on Au electrodes and crystals [14, 39]. The core level N 1s spectra can be fitted to two peaks **(Fig. 3c)**. The peak at 402.6 eV can be assigned to the positively charged nitrogen (N^+) while the one at 400.6 eV can be related to the cation radical $N^{\bullet+}$, both originates from viologen species in the nanocomposite [40]. It can be observed that there is small shift of ~1 eV in the peaks compared to the pristine viologen N 1s band probably due to the interactions with Au/Au_2S nanoparticles within the composite.

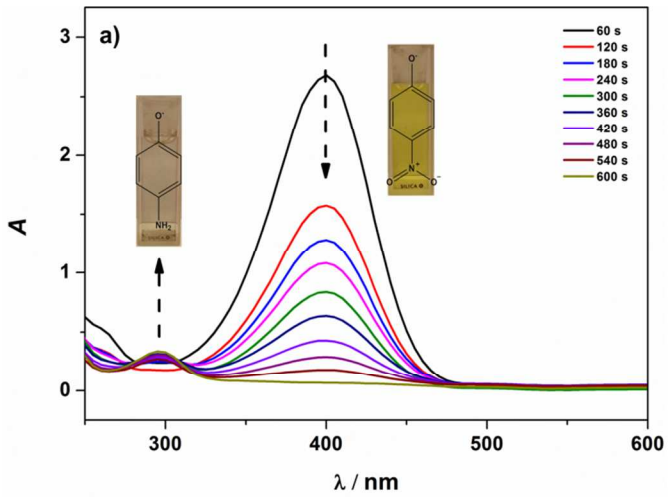

Fig. 4. a) Successive UV-Vis spectra of the reduction of 4-NP by Au/Au_2S-V nanocomposite in presence of excess $NaBH_4$; cuvettes showing change in the color as wells as structural changes before and after the reduction. **b)** Plot of logarithm of absorbance at 400 nm vs. time.

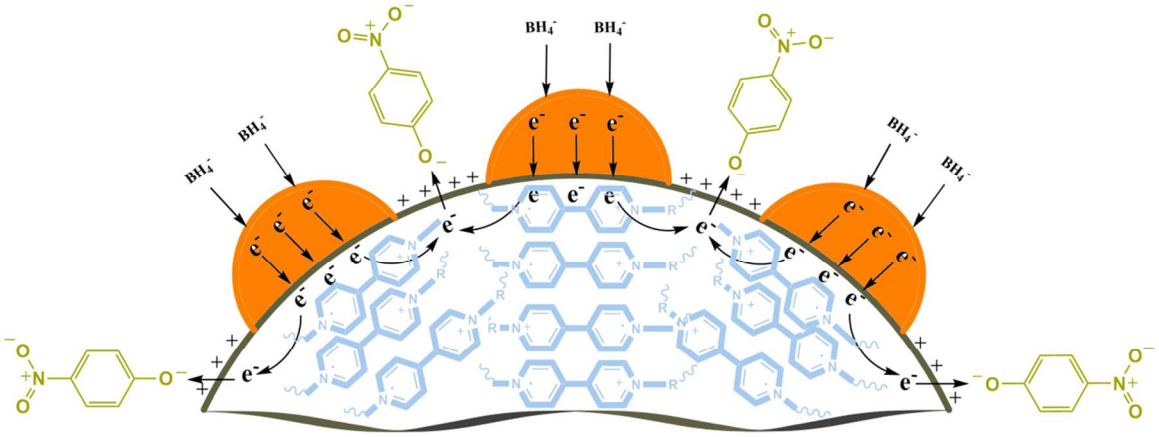

Scheme 2. Mechanistic pathway of 4-NP reduction at the Au/Au_2S surface/ V interface.

The catalytic reduction of 4-NP to 4-AP with an excess amount of $NaBH_4$ has often been used as a model reaction to evaluate the catalyst performance [41]. Herein, we chose this reaction to explore the use of Au/Au_2S-V nanocomposite as catalyst in the reduction of 4-NP. After addition of $NaBH_4$ to 4-NP solution, the color of the solution changed from light yellow to dark yellow, due to formation of 4-nitrophenolate ion. Consequently, the UV-Vis spectrum contains a characteristic absorption peak at 400 nm. Without the catalyst, this peak remains unchanged with time (even after 2 days). When a given amount of Au/Au_2S-V catalyst was added, the reduction process started. The progress of the reaction could be monitored using UV-Vis spectroscopy **(Fig. 4a),** which showed continuous decrease in the absorbance at the wavelength of 400 nm while a new peak emerged at 290 nm assigned to the 4-AP, the reduction product of 4-NP. The reduction process was finished within a time interval of 600 s. At the end of reaction, the peak at 400 nm is no longer observed, indicating the successful reduction of 4-NP to 4-AP in excess of $NaBH_4$ using Au/Au_2S-V composite catalyst. It was found that less than a milligram of catalyst efficiently catalyzes the reduction of 4-NP (20 mol) within a few minutes. For comparison, similar catalytic experiments were performed with only Au/Au_2S nanoparticles and V **(ESI Fig. S1 a,b,c).**

Fig. 4b shows the linear correlation between ln A and reaction time at 293 K, suggesting a pseudo first order reaction. The rate constant (k) at 293 K was calculated from the slope to be 5.95 x 10^{-3} s^{-1} which is a relatively higher value in comparison to the polymer supported Au catalysts [42-47] **(Table 1)**. The activity factor K (k/m; k=rate constant, m=weight of the catalyst) of the Au/Au_2S-V catalyst was calculated to be 11.9 s^{-1} g^{-1}. Our K value is 34 times higher than that reported for spongy Au nanoparticles (0.35 s^{-1} g^{-1}) [48] and more than 5 times larger compared to the highest value reported among the polymer supported Au nanoparticles (2.26 s^{-1} g^{-1}) [34]. Recently, Li et al. reported the highest K value of 31.7 s^{-1} g^{-1} for Au/graphene hydrogel catalyst [49].

Table 1. Reported studies on the reduction of 4-NP over Au/polymer catalysts

Polymer support	Size of Au (nm)	T (K)	NaBH4/4-NP/Au (mol)	k (s^{-1})	Ref
PNIPAM-b-P4VP	2-4	298	167/5/1	1.5×10^{-3}	40
PAEM-PS	1-2	293	1000/1/-	5.1×10^{-1} $m^2.L$	41
PAMAM	2-3	-	1200/1/1	2.0×10^{-3}	42
Poly(VCL-co-AAEM)	-	293	190000/19000/1	4.0×10^{-3}	43
PDMAEMA	4.2	298	28/0.14/1	3.2×10^{-3}	44
Polystyrene	20	298	50/0.27/1	1.6×10^{-4}	45
Viologen	16	293	15000/20/1	5.95×10^{-3}	This work

The superior catalytic activity of as-prepared Au/Au_2S-V nanocomposite can be attributed to the large adsorption of *p*-nitrophenol anion reactants onto the positively-charged V membrane. Moreover, it has been demonstrated that sulfide minerals have strong adsorption and electron donating properties towards removal of organic pollutants [16]. Recently, Kim et al. reported that Fe/FeS nanoparticles can rapidly remove trichloroethylene from water [7]. Therefore, Au_2S nanoparticles would also play similar role in the reduction process of 4-NP. Based on these observations, we propose a detailed mechanistic pathway of catalyzing 4-NP reduction over Au/Au_2S-V composite catalyst **(Scheme 2).** Thus, borohydride ions (BH_4^-) adsorb and transfers electrons to the Au/Au_2S nanoparticle surface. The viologens are very reactive and have the tendency to attract electrons due to their electron accepting ability. Therefore, charge distribution occurs between the Au/Au_2S nanoparticles and adjacent V surface via strong donor-acceptor interactions [50, 51]. Consequently, electrons leave the Au nanoparticles surface and end up in an electron-enriched region at the interface of Au/Au_2S nanoparticles and V adlayer. Meanwhile, the 4-nitrophenolate anion reactants can be easily adsorbed onto the positively charged V due to electrostatic interactions. The presence of surplus electrons along the V surface facilitates the uptake of electrons by the adsorbed 4-NP molecules, which leads to the reduction of 4-NP into the 4-AP. The process continues as the release of 4-AP generates a free active surface and the catalytic cycle can start again.

Conclusions

In conclusion, we have successfully synthesized Au/Au_2S-V hybrid nanocomposite via one step chemical reduction using dithionite. The Au/Au_2S nanoparticles uniformly supported on V molecules assembled as flower like structure. The electron donating ability of Au/Au_2S nanoparticles and the electrostatically assisted greater adsorption of 4-NP molecules on V surface together with donor-acceptor interactions between the two makes Au/Au_2S-V an efficient catalyst in the reduction of nitro-aromatic compounds.

Acknowledgements

All authors gratefully acknowledge financial support from Academy of Finland.

Notes and references

[a] Turku University Centre for Materials and Surfaces (MATSURF), Laboratory of Materials Chemistry and Chemical Analysis, University of Turku, FI-20014 Turku, Finland. *Bhushan Gadgil: bhushan.gadgil@utu.fi, gadgil.bhush@gmail.com, *Carita Kvarnström: carkva@utu.fi
[b] University of Turku Graduate School (UTUGS), FI-20014, Turku, Finland
[c] Laboratory of Materials Science, University of Turku, FI-20014 Turku, Finland.

Electronic Supplementary Information (ESI) available. See DOI: 10.1039/b000000x/

1 R. Averitt, D. Sarkar and N. Halas, *Phys. Rev. Lett.,* 1997, **78,** 4217.
2 B. N. Mbenkum, A. Díaz-Ortiz, L. Gu, P. A. v. Aken and G. Schütz, *J. Am. Chem. Soc.,* 2010, **132,** 10671.
3 S. Sershen, S. Westcott, N. Halas and J. West, *J. Biomed. Mater. Res.,* 2000, **51,** 293.
4 H. Zeng and S. Sun, *Advanced Functional Materials,* 2008, **18,** 391.
5 A. Biswas, O. Aktas, U. Schürmann, U. Saeed, V. Zaporojtchenko, F. Faupel and T. Strunskus, *Appl. Phys. Lett.,* 2004, **84,** 2655.
6 J. Gao, H. Gu and B. Xu, *Acc. Chem. Res.,* 2009, **42,** 1097.
7 E. Kim, J. Kim, A. Azad and Y. Chang, *ACS Applied Materials & Interfaces,* 2011, **3,** 1457.
8 M. Stratakis and H. Garcia, *Chem. Rev.,* 2012, **112,** 4469.
9 B. R. Tagirov, N. N. Baranova, A. V. Zotov, J. Schott and L. N. Bannykh, *Geochim. Cosmochim. Acta,* 2006, **70,** 3689.
10 E. S. Day, L. R. Bickford, J. H. Slater, N. S. Riggall, R. A. Drezek and J. L. West, *Int. J. Nanomedicine,* 2010, **5,** 445.
11 H. Huang, C. Qu, X. Liu, S. Huang, Z. Xu, B. Liao, Y. Zeng and P. K. Chu, *ACS Applied Materials & Interfaces,* 2011, **3,** 183.
12 L. Hirsch, J. Jackson, A. Lee, N. Halas and J. West, *Anal. Chem.,* 2003, **75,** 2377.
13 X. Huang, B. Zhang, L. Ren, S. Ye, L. Sun, Q. Zhang, M. Tan and G. Chow, *J. Mater. Sci. Mater. Med.,* 2008, **19,** 2581.
14 T. Morris, H. Copeland and G. Szulczewski, *Langmuir,* 2002, **18,** 535.
15 A. M. Gobin, E. M. Watkins, E. Quevedo, V. L. Colvin and J. L. West, *Small,* 2010, **6,** 745.
16 J. R. Brown, G. M. Bancroft, W. S. Fyfe and R. A. McLean, *Environ. Sci. Technol.,* 1979, **13,** 1142.
17 R. Gracia and D. Mecerreyes, *Polymer Chemistry,* 2013, **4,** 2206.
18 B. Gadgil, P. Damlin, T. Ääritalo, J. Kankare and C. Kvarnström, *Electrochim. Acta,* 2013, **97,** 378.
19 B. Gadgil, P. Damlin, T. Ääritalo and C. Kvarnström, *Electrochim. Acta,* 2014, **133,** 268.
20 B. Gadgil, E. Dmitrieva, P. Damlin, T. Ääritalo and C. Kvarnström, *Journal of Solid State Electrochemistry,* 2015, **19**, 77.
21 W. Schwarz, I. Shain and E. Kosower, *Journal of the American Chemical Society,* 1961, **83,** 3164.
22 S. Sen, J. Saraidaridis, S. Y. Kim and G. T. R. Palmore, *ACS Applied Materials & Interfaces,* 2013, **5,** 7825.

23 J. Chang, S. Lee, T. Ganesh, R. S. Mane, S. Min, W. Lee and S. Han, *J Electroanal Chem,* 2008, **624,** 167.
24 M. Tagliazucchi, D. B. Tice, C. M. Sweeney, A. J. Morris-Cohen and E. A. Weiss, *ACS Nano,* 2011, **5,** 9907.
25 L. Guerrini, J. V. Garcia-Ramos, C. Domingo and S. Sanchez-Cortes, *Anal. Chem.,* 2009, **81,** 1418.
26 S. Krishnamurthy, I. V. Lightcap and P. V. Kamat, *J. Photochem. Photobiol. A.,* 2011, **221,** 214.
27 N. Kitamura, Y. Nambu and T. Endo, *Journal of Polymer Science Part A: Polymer Chemistry,* 1988, **26,** 993.
28 F. Dong, W. Guo, S. Park and C. Ha, *Chem.Commun.,* 2012, **48,** 1108.
29 M. Wayman and W. Lem, *Canadian Journal of Chemistry,* 1970, **48,** 782.
30 A. Casini, M. C. Diawara, R. Scopelliti, S. M. Zakeeruddin, M. Grätzel and P. J. Dyson, *Dalton Transactions,* 2010, **39,** 2239.
31 G. K. Parker, K. M. Watling, G. A. Hope and R. Woods, *Colloids Surf. Physicochem. Eng. Aspects,* 2008, **318,** 151.
32 Y. Mikhlin, M. Likhatski, A. Karacharov, V. Zaikovski and A. Krylov, *Phys. Chem. Chem. Phys.,* 2009, **11,** 5445.
33 K. Yoshizawa, K. Iwahori, K. Sugimoto and I. Yamashita, *Chem. Lett.,* 2006, **35,** 1192.
34 K. Kuroda, T. Ishida and M. Haruta, *Journal of Molecular Catalysis A: Chemical,* 2009, **298,** 7.
35 N. Wang, P. Damlin, B. M. Esteban, T. Ääritalo, J. Kankare and C. Kvarnström, *Electrochim. Acta,* 2013, **90,** 171.
36 D. Wierse, M. Lohrengel and J. Schultze, *Journal of Electroanalytical Chemistry and Interfacial Electrochemistry,* 1978, **92,** 121.
37 D. Rathod, S. Warren, K. Keane, D. A. Egan and E. Dempsey, *Analytical Methods,* 2011, **3,** 799.
38 F. Lu, F. Chang, M. G. Mohamed, T. Liu, C. Chao and S. Kuo, *Journal of Materials Chemistry C,* 2014, **2**, 6111.
39 C. Vericat, M. E. Vela, G. Corthey, E. Pensa, E. Cortes, M. H. Fonticelli, F. Ibanez, G. E. Benitez, P. Carro and R. C. Salvarezza, *RSC Adv.,* 2014, **4,** 27730.
40 L. Cao, M. Mou and Y. Wang, *Journal of Materials Chemistry,* 2009, **19,** 3412.
41 K. Esumi, R. Isono and T. Yoshimura, *Langmuir,* 2004, **20,** 237.
42 Y. Wang, G. Wei, W. Zhang, X. Jiang, P. Zheng, L. Shi and A. Dong, *Journal of Molecular Catalysis A: Chemical,* 2007, **266,** 233.
43 M. Schrinner, F. Polzer, Y. Mei, Y. Lu, B. Haupt, M. Ballauff, A. Göldel, M. Drechsler, J. Preussner and U. Glatzel, *Macromolecular Chemistry and Physics,* 2007, **208,** 1542.
44 H. Wu, Z. Liu, X. Wang, B. Zhao, J. Zhang and C. Li, *J. Colloid Interface Sci.,* 2006, **302,** 142.
45 A. Pich, A. Karak, Y. Lu, A. K. Ghosh and H. P. Adler, *Journal of Nanoscience and Nanotechnology,* 2006, **6,** 3763.
46 M. Zhang, L. Liu, C. Wu, G. Fu, H. Zhao and B. He, *Polymer,* 2007, **48,** 1989.
47 S. Panigrahi, S. Basu, S. Praharaj, S. Pande, S. Jana, A. Pal, S. K. Ghosh and T. Pal, *The Journal of Physical Chemistry C,* 2007, **111,** 4596.
48 M. H. Rashid, R. R. Bhattacharjee, A. Kotal and T. K. Mandal, *Langmuir,* 2006, **22,** 7141.
49 J. Li, C. Liu and Y. Liu, *Journal of Materials Chemistry,* 2012, **22,** 8426.
50 H. Li, D. Chen, Y. Sun, Y. B. Zheng, L. Tan, P. S. Weiss and Y. Yang, *J. Am. Chem. Soc.,* 2013, **135,** 1570.
51 M. Hao, X. Liu, M. Feng, P. Zhang and G. Wang, *J. Power Sources,* 2014, **251,** 222.